Available online at www.sciencedirect.com

ScienceDirect

www.elsevier.com/locate/jes

JES JOURNAL OF ENVIRONMENTAL SCIENCES

www.jesc.ac.cn

Effects of sludge characteristics on electrical resistance and energy consumption during electro-dewatering process

Li Sha[1], *Xiaoyan Yu*[2], *Zhangxiang Wu*[1], *Xingxin Liu*[1], *Shuting Zhang*[1,*]

[1] *School of Environmental Science and Engineering, Tianjin University, Tianjin 300354, China*
[2] *School of Environmental and Safety Engineering, Taiyuan Institute of Technology, Taiyuan 030008, China*

ARTICLE INFO

Article history:
Received 5 July 2020
Revised 19 August 2020
Accepted 1 September 2020
Available online 11 September 2020

Keywords:
Sludge
Electro-dewatering
Electrical resistance
Energy consumption
Multiple linear regression

ABSTRACT

The increase of electrical resistance (ER) and energy consumption (EC) during the later stage of dewatering is a major problem hindering the development of electro-dewatering (EDW) technology. As the variations of sludge characteristics are significant during the EDW process, the relationships between sludge characteristics and ER and EC during EDW remain unclear. In this study, the effects of moisture content (MC), thickness, pH, conductivity, zeta potential, temperature, and gas volume on the ER and EC during the EDW process were statistically investigated using correlation and multiple linear regression analyses. Herein, the results showed that the ER of the sludge near the anode was primarily affected by pH, whereas the sludge near the cathode was primarily affected by the MC and conductivity. Further, sludge temperature and conductivity were the most reliable indicators to predict the EC near the anode and cathode, respectively. The results of this study provide theoretical guidance useful for solving the increase of ER and EC during the later stage of the EDW process.

Introduction

Wastewater treatment plants (WWTPs) produce large volumes of sewage sludge with different characteristics during biological processes. As sewage sludge contains water, it has a high cost of transport and disposal (Citeau et al., 2011). Thus, to reduce costs, it is necessary to remove as much water as possible. Currently, in China, sludge with a moisture content (MC) higher than 60% is not permitted for further disposal (Sheng et al., 2010). To date, mechanical dewatering methods widely used in WWPTs, such as filtration-compression and centrifugation, can only reduce the MC of sludge to approximately 80% (Cai et al., 2016). Therefore, even after mechanical dewatering, sludge must be further dewatered by deep dewatering methods (Sha et al., 2020; Guo et al., 2018).

Electro-dewatering (EDW) is considered to be an efficient deep dewatering method of sludge. EDW technology can drive the liquid with part of positive charges from anode to cathode to ultimately decrease the MC of sludge to 30% (Li et al., 2018; Yang et al., 2018). EDW is attracting increasing attention due to its low energy consumption (EC). Mahmoud et al. reported that EDW could cut EC by 10% – 25% to achieve a MC of 68% – 40%, as compared with thermal drying (Mahmoud et al., 2011).

However, there are still some problems regarding the development of the EDW process, including the increase of electrical resistance (ER) and EC at the later stage of dewatering (Citeau et al., 2016; Conrardy et al., 2016). The EDW

* Corresponding author.
E-mail: zhangst@tju.edu.cn (S. Zhang).

https://doi.org/10.1016/j.jes.2020.09.001
1001-0742/

system is essentially an electrochemical reactor (Mahmoud et al., 2018), wherein electrophoresis, electroosmosis, electromigration, and electrolysis reactions occur during its processes (Mahmoud et al., 2010). These reactions cause variation in sludge characteristics from the anode to the cathode, which can affect the ER and EC. To date, many researchers have studied the influence of some sludge characteristics on ER and EC during the EDW process. In a study regarding ER, Yu et al. reported that the increase in ER was mainly due to the decrease of sludge MC near the anode (Yu et al., 2017). Citeau et al. pointed out that sludge ER was related to ionic concentration (Citeau et al., 2012). Moreover, Mahmoud et al. proposed that sludge thickness, MC, pH, electro-migration, conductivity, and gas could affect the sludge ER near the anode (Conrardy et al., 2016). Regarding EC, Lv et al. found that the migration of soluble ions caused an excessive EC (Lv et al., 2020). Wu et al. reported that EC was proportional to sludge thickness (Wu et al., 2019), and Citeau et al. revealed that changes in particle surface charge affected the EC (Citeau et al., 2011). Further, Navab-Daneshmand et al. proposed that the EC increased rapidly due to the large current under conditions of high conductivity (Navab-Daneshmand et al., 2015).

While researches on the sludge characteristics, ER, and EC are extensive, studies regarding the relationships between them are still lacking. Therefore, it is essential for the development of the EDW process to study these relationships. Conventional correlation and regression analyses are convenient and simple approaches used to evaluate these relationships (Wu et al., 2020). Correlation and multiple linear regression analyses have been applied across environmental fields to explore the coupling effects and complex interaction amongst many physiochemical factors (Fazeli Sangani et al., 2019). Bai et al. employed a regression analysis to evaluate the sludge properties related to EDW efficiency, showing that the presence of extracellular polymeric substances was the most significant deleterious factor (Bai et al., 2019). Wu et al. (2020) adopted correlation and multiple linear regression analyses to explore the relationship between dewatering performance and sludge/sediment properties in EDW. However, scarcely researches used correlation and multiple regression analyses to evaluate the effects of sludge characteristics on ER and EC during EDW process.

Therefore, this study systematically investigated the effects of sludge characteristics on ER and EC during the EDW process using correlation and multiple linear regression analyses. Herein, theoretical guidance for solving the high ER and high EC at the later stage of the EDW process was provided. The objectives of this study were: (1) to explore the effects of sludge characteristics on ER and EC; (2) to explore the relationship between sludge characteristics and ER and EC; and (3) to determine the primary factors that affect ER and EC during the EDW process.

1. Materials and methods

1.1. Sludge

The raw sludge used in this study was obtained from the centrifugal dewatering units of the Xianyang Road Wastewater Treatment Plant in Tianjin (China). The sludge samples were stored at 4°C before testing, and all the tests were completed within a week. The main characteristics of raw sludge are summarized in Table 1.

Table 1 – Main characteristics of raw sludge.

Parameters	Measured values
MC	85.76%±0.13%
VS/TS	51.04%±1.03%
pH	7.22±0.05
Zeta potential	-17.00±0.28 mV
Conductivity	641.50±28.99 μS/cm
Temperature	17.30±0.85°C

1.2. Experimental set-up

As shown in Fig. 1a, the experimental set-up for EDW mainly included a dewatering unit and a direct current (DC) stabilized power unit. The reactor of the dewatering unit was made of polytetrafluoroethylene (PTFE) (75 mm inner diameter and 50 mm height), and the reactor had three slits (1 mm width) from top to bottom. A PTFE external jacket was added at the top of the cylinder to guarantee the mechanical resistance. An upper circular anode was made of ruthenium coated titanium and was placed against the piston head. A lower circular cathode was placed under a filter cloth (40 μm thickness and 44 μm pore size), both of which were stainless steel. The cathode and filter cloth were held by a hollow circular tray made of PTFE that could be fixed to the cylinder. The anode and cathode electrodes were connected to a DC stabilized power source (maximum 60 V and 20 A, DH1716A-10, China). The filtrate was collected in a beaker and an electronic balance was set under the beaker to monitor the quality of the filtrate.

1.3. EDW tests

A series of EDW tests using 160 g raw sludge were conducted under a constant voltage (40 V) and pressure (1 bar). The initial thickness of the sludge cake was 32 mm. As shown in Fig. 1b, the sludge cake was evenly divided into four horizontal layers. The initial weight and thickness of sludge cake in each layer were 40 g and 8 mm, respectively. A movable titanium circular grid used as an extra electrode and a movable thermocouple were located in the PTFE cylindrical chamber to measure the voltage and temperature (Fig. 1c). They were connected to an external monitoring device by soft connectors via the slits of the reactor. The operation steps for placing sludge into the reactor are summarized in the Supporting information, and the ER calculation methods of each layer were derived from Conrardy et al. (2016). During the EDW process, voltage, current, filtrate quality, and sludge temperature were measured. When the filtrate flow rate was less than 0.05 g/min for 5 min, the dewaterability limit of sludge was considered to be reached (Yu et al., 2017). In this study, it took approximately 46 min to reach the dewaterability limit. At intervals of 2, 4, 6, 8, 10 , 14, 18, 22, 30, 38, and 46 min, the dewatered sludge cake of each layer was taken from the reactor to measure other in-

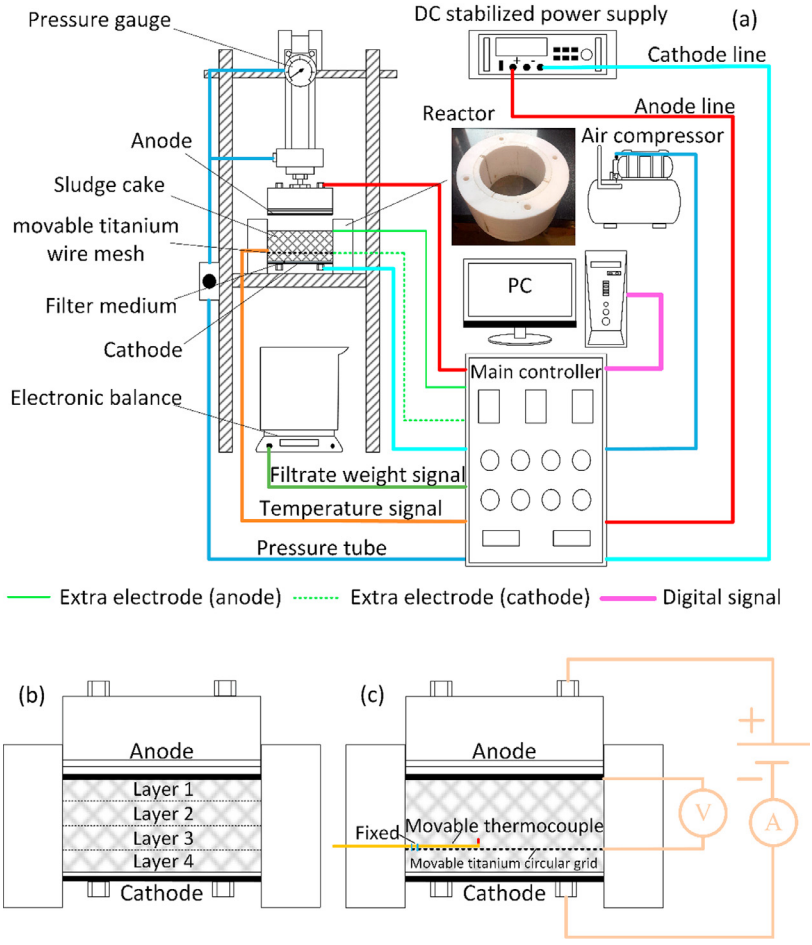

Fig. 1 – The schematic of EDW experimental procedures: (a) the EDW experimental set-up, (b) schematic of sludge layers and (c) reactor using the movable measurement electrode and the movable thermocouple.

dicators (e.g., MC, thickness, pH, conductivity, and zeta potential).

1.4. *Analysis methods*

The MC and volatile solid (VS) were determined by heating the sludge samples to 105°C for 24 hr and 550°C for 4 hr, respectively (Sha et al., 2019). The thickness of sludge cake was measured using a Vernier caliper (accuracy: 0.1 mm), and the pH and conductivity were determined as reported by Li et al. (2018). The digital pH meter (PHBJ-260, Rex, China) and the conductivity meter (DDB-303A, Rex, China) were used to measure the pH and conductivity values in the supernatant suspension with a sludge to water ratio of 1:10. For the zeta potential analysis, 5 g sludge samples were mixed in 50 mL deionized water for 24 hr to prepare a suspension. Then, the zeta potential was determined by zeta potential analyzer (zetasizer nano ZS90, Malvern, UK).

1.5. *Governing equations*

The ER (R, Ω) of the sludge during the EDW process was calculated using Ohm's law:

$$R = \frac{U}{I} \tag{1}$$

Where U (V) is the voltage drop of sludge, and I (A) is the current intensity.

The EC (P, kWh/kg$_{dewater}$) at each layer was calculated as follows:

$$P = \frac{\int IR^2 dt}{m_{dewater}} \tag{2}$$

where $m_{dewater}$ (kg) is the mass of filtrate removed.

The electrochemical reactions occur at the electrode surface. The possible electrode reactions are as follows (Mahmoud et al., 2010):

At the anode:

$$2H_2O - 4e^- \rightarrow O_2 \uparrow + 4H^+ \; E_0 = 1.229V \tag{3}$$

At the cathode:

$$2H_2O + 2e^- \rightarrow H_2 \uparrow + 2OH^- \; E_0 = -0.828V \tag{4}$$

According to the principle of charge conservation, a relationship between oxygen production of layer 1 (Q_{gas}) and the electricity quantity of the EDW process was calculated as follows (Yang et al., 2018):

$$Q_{gas} = \frac{Q_e}{4eN_A} \tag{5}$$

Table 2 – Summary of correlation analysis of electrical resistance and sludge characteristics.

Sludge characteristics (x)	Fitting equations	Layer	Coefficient a	Coefficient b	Coefficient c	Adj. R^2	P
MC	$R = ae^{(\frac{b}{x})} + c$	1	0.038	3.661	0.169	0.018	>0.05
		2	0.656	1.384	0.342	0.990	<0.01
		3	1.521×10^{-12}	14.869	5.060	0.986	<0.01
		4	1.863×10^{-8}	12.158	3.617	0.860	<0.01
Thickness	$R = ae^{(\frac{b}{x})} + c$	1	3.709×10^{-8}	52.765	8.372	0.996	<0.01
		2	0.306	5.939	3.438	0.991	<0.01
		3	6.608×10^{-5}	19.786	5.192	0.990	<0.01
		4	9.916×10^{-6}	40.343	3.814	0.878	<0.01
pH	$R = ae^{(\frac{b}{x})} + c$	1	2.207×10^{-5}	46.862	7.212	0.984	<0.01
		2	2.406×10^{-12}	187.001	4.044	0.993	<0.01
		3	3.072×10^{-14}	237.553	2.854	0.676	<0.01
		4	1.489×10^{12}	-253.264	3.786	0.917	<0.01
Conductivity	$R = ae^{(\frac{b}{x})} + c$	1	4.762×10^{10}	-26780.761	8.064	0.972	<0.01
		2	3.141×10^{6}	-10378.701	4.784	0.991	<0.01
		3	1.742×10^{-5}	2996.080	4.971	0.924	<0.01
		4	6.225×10^{-7}	4569.134	3.966	0.936	<0.01
Zeta potential	$R = ax + b$	1	3.308	53.810	-	0.372	<0.05
		2	-20.540	364.143	-	0.396	<0.05
		3	-0.495	-0.621	-	-0.099	>0.05
		4	-0.904	-13.195	-	0.585	<0.01
Temperature	$R = ax + b$	1	0.576	-8.026	-	0.054	>0.05
		2	0.264	-3.271	-	0.073	>0.05
		3	0.071	4.040	-	-0.040	>0.05
		4	0.047	2.892	-	-0.018	>0.05
Gas volume	$R = ae^{(\frac{b}{x})} + c$	1	1.567×10^{22}	-9299.418	9.017	0.797	<0.01

where Q_{gas} (mol) is the oxygen production, N_A (6.02×10^{23}) is Avogadro's constant, e (1.60×10^{-19} C) is the elementary charge, and Q_e (C) is the electricity quantity of the EDW process as given by:

$$Q_e = \int_0^t I dt \tag{6}$$

where t (sec) is the dewatering time, and I (A) is the current.

The theoretical oxygen emission volume (V_{o_2}) was calculated as follows:

$$V_{o_2} = \frac{Q_{gas} RT}{P} \tag{7}$$

where V_{o_2} (m^3) is the theoretical oxygen emission volume, T (K) is the thermodynamic ideal gas temperature, R (8.314 J/(mol K)) is the gas constant, and P (Pa) is the gas pressure.

According to the Helmholtz-Smoluchowski equation, the electroosmotic flow rate (υ) is as follows (Mahmoud et al., 2010):

$$\vec{\upsilon} = \frac{D\zeta}{4\pi\mu} \nabla\varphi \tag{8}$$

where D (F/m) is the dielectric constant of liquid, ζ (mV) is the zeta potential, $\nabla\varphi$ is (V/m) the electric field intensity, and μ (Pa•sec) is the fluid viscosity.

As shown in Figs. 3 and 4a-i, the ER (R) has a good correlation with the MC, thickness, pH, conductivity, and gas volume. This correlation can be expressed as follows:

$$R = ae^{\left(\frac{b}{x}\right)} + c \tag{9}$$

where a, b, and c are coefficients (Table 2), and x is the MC, thickness, pH, conductivity, or gas volume.

The correlation between the ER (R), zeta potential, and temperature is expressed as:

$$R = ax + b \tag{10}$$

where a and b are coefficients (Table 2) and x is the zeta potential or temperature.

In addition, a linear relationship was also observed between the EC (P) and sludge characteristics, including MC, thickness, pH, conductivity, zeta potential, temperature, and gas volume (Figs. 4b and 5). This relationship is represented as:

$$P = ax + b \tag{11}$$

where a and b are coefficients (Table 3) and x is the MC, thickness, pH, conductivity, zeta potential, temperature, or gas volume.

1.6. *Statistical analysis*

A regression analysis was conducted using SPSS 21.0 (IBM, USA). With a backward elimination procedure, the analysis obtained statistically significant variables ($p < 0.05$). A stepwise multiple linear regression (SMLR) was used to determine the most reliable factors. The regression equation is shown as follows (Wu et al., 2020):

$$Y = \sum_{G=1}^{G} X_G \beta_G + \varepsilon \tag{12}$$

Table 3 – Summary of correlation analysis of energy consumption and sludge characteristics.

Sludge characteristics (x)	Fitting equations	Layer	Coefficient *a*	Coefficient *b*	Adj. R^2	*P*
MC	$P = ax + b$	1	-3.221	2.689	0.980	<0.01
		2	-0.650	0.677	0.380	<0.05
		3	-1.281	1.123	0.849	<0.01
		4	-2.167	1.813	0.891	<0.01
Thickness	$P = ax + b$	1	-0.177	1.177	0.688	<0.01
		2	-0.070	0.519	0.560	<0.01
		3	-0.083	0.579	0.772	<0.01
		4	-0.116	0.772	0.737	<0.01
pH	$P = ax + b$	1	-0.249	1.740	0.906	<0.01
		2	-0.233	1.878	0.351	<0.05
		3	-0.424	3.381	0.272	<0.05
		4	0.223	-1.675	0.796	<0.01
Conductivity	$P = ax + b$	1	0.002	-1.327	0.900	<0.01
		2	-2.348×10^{-4}	0.107	-0.053	>0.05
		3	-8.812×10^{-4}	0.625	0.872	<0.01
		4	-0.001	0.826	0.893	<0.01
Zeta potential	$P = ax + b$	1	0.050	1.007	0.866	<0.01
		2	0.197	3.633	0.299	<0.05
		3	-0.213	-3.525	0.237	>0.05
		4	-0.058	-0.937	0.813	<0.01
Temperature	$P = ax + b$	1	0.013	-0.230	0.983	<0.01
		2	0.007	-0.133	0.924	<0.01
		3	0.007	-0.143	0.876	<0.01
		4	0.009	-0.211	0.802	<0.01
Gas volume	$P = ax + b$	1	0.005	0.064	0.974	<0.01

where the independent variable, X, is the sludge characteristic, Y denotes the dependent variable of ER (R) or EC (P), β represents the regression coefficients, and ε is the intercept.

The performance of these developed equations were assessed using an adjusted coefficient of determination (adj. R^2) (Zheng et al., 2020). The adj. R^2 is a modified version of R^2, which indicates the goodness of fit of a developed equation. Differences with p values of less than 0.05 were considered significant.

2. Results and discussion

2.1. ER and EC

As shown in Fig. 2a, the sludge ER of each layer stayed below 15 Ω during the initial 30 min. Then, the ER increased across the cake from cathode to anode. When the dewaterability limit was reached, the ER of layers 1, 2, 3, and 4 were 138.29 ± 2.23 Ω, 56.30 ± 1.13 Ω, 28.38 ± 0.91 Ω, and 15.96 ± 0.91 Ω, respectively. These results indicate that the ER near the anode increased sharply at the later stage of the EDW process. Conrardy et al. (2016) pointed out that this could be due to the migration and interaction of ions (mainly H^+), the decrease of MC, and presence of gas.

As shown in Fig. 2b, the EC of layer 1 increased sharply with increasing time and reached 1.06 ± 0.08 $kWh/kg_{dewater}$ at 30 min. The EC of layers 2, 3, and 4 showed a fluctuating increasing trend when the dewatering time increased to 22 min. After 22 min, the EC of the layers 3 and 4 remained relatively flat, and the EC of layer 2 decreased significantly in the last 8 min of dewatering. These results indicate that the EC of layer 1 was higher than that of other layers during the EDW process.

2.2. Correlation analysis

2.2.1. ER and sludge characteristics

As shown in Fig. 3a-i, the ER of the sludge was less than 20 Ω when the MC of the four layers decreased from 85.76% ± 0.13% to 60%, and then the ER increased across the cake from cathode to anode. The ER of layers 2, 3, and 4 increased with decreasing MC, showing good correlations between ER and MC (layer 2: adj. $R^2 = 0.990$, $p < 0.01$; layer 3: adj. $R^2 = 0.986$, $p < 0.01$; layer 4: adj. $R^2 = 0.860$, $p < 0.01$) (Table 2). These results are consistent with previous reports (Wu et al., 2019). Note that layer 1 differed from the other layers as the MC of layer 1 increased slightly after 30 min (Fig. 3a-ii). However, the ER of layer 1 still increased sharply and became the greatest of the four layers (Fig. 2a). Notably, the MC of layer 1 had a bad correlation with the ER (adj. $R^2 = 0.018$, $p > 0.05$), indicating that the decrease of MC was not the main factor influencing the ER of layer 1.

As shown in Fig. 3b-i and Table 2, the thickness of the four layers and the ER correlated well during the EDW process (adj. R^2: 0.878 – 0.996, $p < 0.01$). When the thickness decreased below 3 mm, the ER began to increase. Note that thickness decreased with dewatering time (Fig. 3b-ii) due to the decrease of MC. This decreasing MC could gradually change the passing paths of electrical current from liquid to solid phases. When the low conductivity solid path became the main passing path of electrical current, the ER increased (Mahmoud et al., 2018).

As shown in Fig. 3c-i and Table 2, the pH of the four layers had a significant influence on ER (adj. R^2: 0.676 – 0.993, $p <$

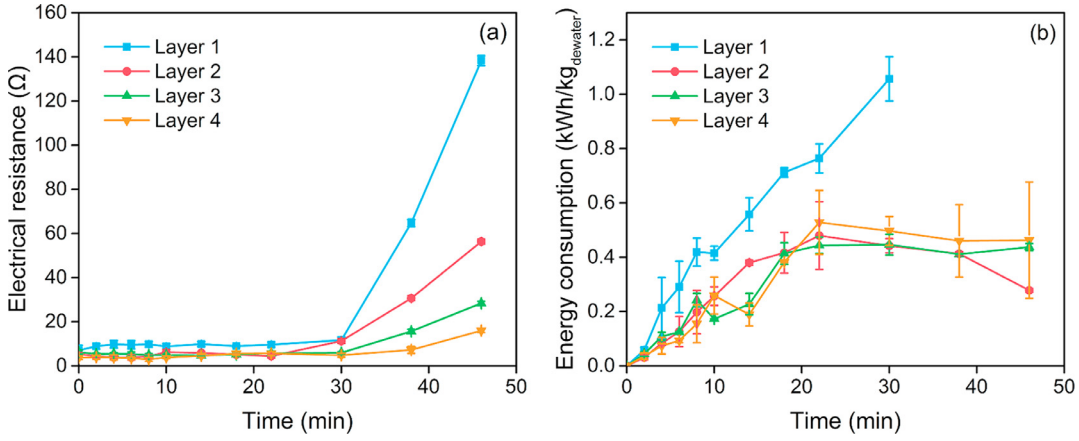

Fig. 2 – Variations of (a) electrical resistance and (b) energy consumption of four layers during EDW process.

0.01). In layers 1, 2, and 3, the pH decreased with dewatering time (Fig. 3c-ii), and the ER clearly increased with the decrease of pH after 30 min (Fig. 3c-i). Particularly, the ER of layer 1 increased sharply when the pH was less than 3.58 ± 0.05. The pH of the three upper layers decreased because the rate of H^+ diffusion toward the cathode was 1.8 times that of OH^- towards the anode (Wu et al., 2020). Compared with the obvious decrease in pH of layers 1 and 2, the pH of layer 3 changed slightly until it became neutral, which occurred as most of the H^+ and OH^- reacted in layer 3. The H^+ near the anode tended to interact with the anionic chemical groups present on the solids surface to constitute non-ionic chemical systems, which were poor electric conductors (Conrardy et al., 2016), leading to the increase of ER. Conversely, the ER of layer 4 began to increase obviously with increasing pH after 30 min, which was a result of the OH^- combining with substances, such as Ca, Mg, and Fe, to constitute a non-ionic chemical system.

As shown in Fig. 3d-i and Table 2, the ER of the layers were strongly correlated to the sludge conductivity (adj. R^2: 0.924 – 0.991, $p < 0.01$). Note that, after 30 min, the ER of layers 1 and 2 increased significantly with increasing conductivity, whereas the ER of layers 3 and 4 increased with decreasing conductivity. At the anode side, the increased conductivity of layers 1 and 2 at the later stage of the EDW process (Fig. 3d-ii) is due to the formation of H^+ in according to Eq. (3) (Deng et al., 2020). However, as previously mentioned, H^+ tended to interact with the anionic chemical groups to constitute non-ionic chemical systems, thereby increasing the ER. At the cathode side, the decrease in conductivity of layers 3 and 4 meant a decrease of ion concentration in the solution (Tafti et al., 2015), which could increase the ER.

As shown in Fig. 3e-i and Table 2, the ER had poor correlation with the zeta potential for all four layers. This indicates that the zeta potential had little direct bearing on the ER. According to Eq. (8), the zeta potential affected the direction and speed of electroosmotic flow. When the zeta potential was below 0 mV, the direction of electroosmotic flow was from the anode to the cathode (Yeung et al., 1997). After 30 min, the zeta potential of layer 1 changed from negative to positive (Fig. 3e-ii), which reversed the electroosmosis driving force close to the anode causing the electroosmotic flow of layer 1 to move toward the anode, which led to the increase of MC in layer 1 after 30 min. The sludge of layer 2 continued to dewater without the moisture supplement from layer 1, resulting in the lowest MC of layer 2 at the dewaterability limit (Fig. 3a-ii).

As shown in Fig. 3f-i and Table 2, there is no evident regularity between the temperature due to Joule heating and the ER. This suggests that temperature was not the main factor influencing the ER. Moreover, it could be seen in Fig. 3f-ii that the temperature of the layers increased during the initial 30 min and then decreased. The maximum temperature of layers 1, 2, 3, and 4 reached 96.10 ± 3.25°C, 91.10 ± 1.70°C, 88.50 ± 7.78°C, and 82.20 ± 5.37°C, respectively. This is consistent with previous reports as temperature at the anode side was higher than that at the cathode side during the later stage of the EDW process (Zhang et al., 2017). Increasing temperatures (more than 40°C) could destroy microbial cells and cause the disintegration of extracellular polymeric substances (EPS) to release water (Deng et al., 2019; Lv et al., 2019). Further, increasing temperature could decompose the thermally labile samples and form gas bubbles (Tang et al., 2004), which are detrimental to conduction.

As shown in Fig. 4a-i and Table 2, the ER had a good correlation with the theoretical gas emission volume (adj. $R^2 = 0.797$, $P < 0.01$), increasing sharply when the gas volume increased to 188.62 ± 5.60 mL. Fig. 4a-ii show how the gas volume increased with time. As gas accumulated between the sludge cake and the plate anode, a gas barrier layer formed at the later stage of the EDW process, thereby increasing the ER of layer 1(Yang et al., 2018).

2.2.2. *EC and sludge characteristics*

As shown in Fig. 5a and Table 3, the EC of layers 1 (adj. $R^2 = 0.980$, $p < 0.01$), 3 (adj. $R^2 = 0.849$, $p < 0.01$) and 4 (adj. $R^2 = 0.891$, $p < 0.01$) showed significant correlations with MC, and the EC increased with the decrease of MC. The MC of sludge cake decreased with the removal of moisture. Generally, low MC made dewatering more difficult. The decrease of MC could lead to poor dewaterability and increase the EC

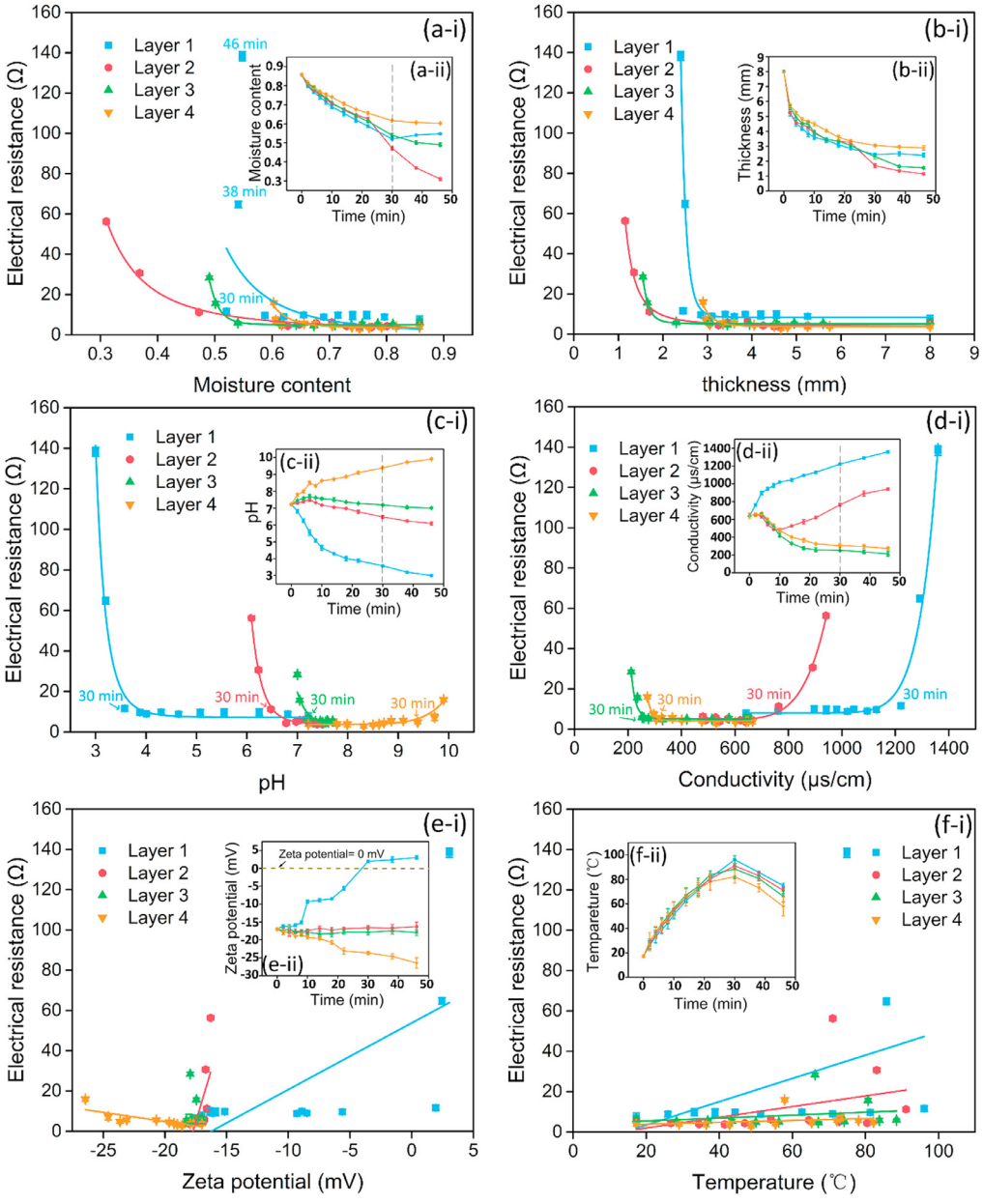

Fig. 3 – Correlations between the electrical resistance and sludge characteristics: (a-i) MC, (b-i) thickness, (c-i) pH, (d-i) conductivity, (e-i) zeta potential and (f-i) temperature; variations of sludge characteristics during EDW process: (a-ii) MC, (b-ii) thickness, (c-ii) pH, (d-ii) conductivity, (e-ii) zeta potential and (f-ii) temperature.

(Wu et al., 2020). However, the EC decreased when the MC of layer 2 was less than 60%. The results were related to the rapid decrease of MC in layer 2 (Fig. 3a-ii). The rapid decrease of MC meant the increase of the dewaterability, which led to the decrease of EC.

As shown in Fig. 5b and Table 3, the EC exhibited middle coefficients of correlation with sludge thickness of four layers (adj. R^2 = 0.560 – 0.772, $p < 0.01$). The sludge thickness was related to MC, therefore a decreasing sludge thickness meant decreasing MC. As previously mentioned, a decreasing MC led to increasing EC. In addition, Wu et al. found that during the EDW process, the sludge thickness decreased, and the electric field strength increased, resulting in the increase of EC (Wu et al., 2019).

As shown in Fig. 5c and Table 3, the EC had a significant positive correlation with the pH of layers 1 (adj. $R^2 = 0.906$, $p < 0.01$) and 4 (adj. $R^2 = 0.796$, $p < 0.01$), respectively, and small correlations with the pH of layers 2 (adj. $R^2 = 0.351$, $p < 0.05$) and 3 (adj. $R^2 = 0.272$, $p < 0.05$), respectively. The pH of layer 1 decreased during the EDW process, and this lower pH inhibited dehydration which caused it's a decline of the dewatering performance and an increase in EC (Wei et al., 2020; Wu et al., 2020). The pH of layers 2 and 3 did not change significantly during the EDW process (Fig. 3c-ii), which suggests that it might

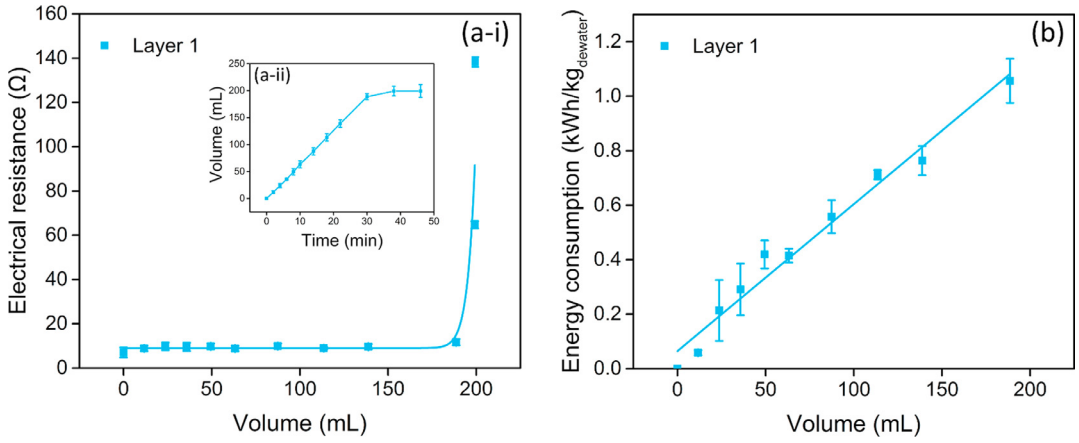

Fig. 4 – (a-i) Correlation between the electrical resistance and gas volume; (a-ii) variation of gas volume during EDW process; (b) correlation between the energy consumption and gas volume.

not be the main factor increasing the EC. With the dewatering time increased, the pH of layer 4 increased (Fig. 3c-ii) and gradually moved away from the isoelectric point, which corresponds to a zeta potential of 0 mV, was between 3.58 and 3.88 in this study. Navab-Daneshmand et al. (2015) reported that at pH values far from the isoelectric point, high charge densities enhanced repulsion and therefore, expanded the matrix. The resultant expanded structure would present a higher resistance to flow, thereby decreasing the dewatering efficiency and increasing the EC.

As shown in Fig. 5d and Table 3, the EC significantly correlates with the conductivity of layers 1 (adj. $R^2 = 0.900, p < 0.01$), 3 (adj. $R^2 = 0.872, p < 0.01$), and 4 (adj. $R^2 = 0.893, p < 0.01$). The EC increased with increasing conductivity in layer 1 (Fig. 3d-ii), where a higher conductivity of sludge caused a higher current density, which led to a greater EC (Wei et al., 2020; Wu et al., 2020). Conversely, the low conductivity of layers 3 and 4 made it difficult for the EDW process hard to remove water (Lv et al., 2018), resulting in an increase of EC. Note that the EC had no significant effect from the conductivity of layer 2 (adj. $R^2 = -0.053, p > 0.05$), indicating that conductivity had no influence on EC in layer 2.

As shown in Fig. 5e and Table 3, the EC significantly correlated with the zeta potential of layers 1 (adj. $R^2 = 0.866, p < 0.01$) and 4 (adj. $R^2 = 0.813, p < 0.01$). The zeta potential of layer 1 showed a fluctuating increasing trend with time (Fig. 3e-ii). According to the Eq. (8), the increase of the zeta potential of layer 1 decreased the electroosmotic flow rate and the amount of water removed, resulting in an increase in EC. Moreover, the decreasing zeta potential of layer 4 could increase the electroosmotic flow rate and promote the EDW, however, the EC also increased. This increase could be due to other factors having a greater influence than zeta potential on EC. The EC had low coefficients of correlation with the zeta potential of layer 2 (adj. $R^2 = 0.299, p < 0.05$), and no correlation with the zeta potential of layer 3 (adj. $R^2 = 0.237, p > 0.05$). These results indicate that the zeta potential of layers 2 and 3 had little influence on the EC.

As shown in Fig. 5f and Table 3, the EC significantly correlated with the temperature of the four layers (adj. $R^2 = 0.802 - 0.983, p < 0.01$), increasing with increasing temperature. The Joule heating generated during the EDW process significantly increased the temperature of the sludge cake and consequently decreased the liquid viscosity, forcing the water out of the solid capillaries (Mahmoud et al., 2018). However, with decreasing MC, the dewatering process becomes more difficult, and the EC could increase.

As shown in Fig. 4b and Table 3, the EC also significantly correlated with the theoretical gas emission volume (adj. $R^2 = 0.974, P < 0.01$). The gas barrier layer formed between the flat anode plate and the sludge of layer 1 hindered the contact with each other, thereby reducing the EDW efficiency and thus increasing the EC. This indicates that the gas volume had a great influence on the EC.

2.3. *Multiple linear regression analysis*

Backward elimination multiple linear regression (BEMLR) and SMLR were used to assess the quantitative relationships for ER (R) and EC (P) by establishing regression equations.

2.3.1. *ER*

Sludge characteristics with a high adj. R^2 (MC, thickness, pH, conductivity, and gas volume) were selected for the BEMLR and SMLR analyses of the ER (R). Note that the non-linear equations were converted into linear equations before BEMLR and SMLR analysis. The regression equations of BEMLR were outlined as follows:

Layer 1:

$$R = 8.7926 - \left(5.4819 \times 10^{-9}\right) \times e^{\frac{52.765}{H}} + \left(4.6572 \times 10^{10}\right) \times e^{-\frac{26780.761}{C}} + \left(3.4494 \times 10^{21}\right) \times e^{-\frac{9299.418}{V}} \quad (13)$$

Layer 2:

$$R = 4.1365 + 0.1512 \times e^{\frac{5.939}{H}} + \left(1.5978 \times 10^{10}\right) \times e^{-\frac{10378.701}{C}} \quad (14)$$

Layer 3:

$$R = 5.0904 + \left(1.1572 \times 10^{-12}\right) \times e^{\frac{14.869}{MC}} - 0.0031 \times e^{\frac{19.786}{H}} + \left(6.3007 \times 10^{-15}\right) \times e^{\frac{237.553}{pH}} + \left(4.0815 \times 10^{-6}\right) \times e^{\frac{2996.080}{C}} \quad (15)$$

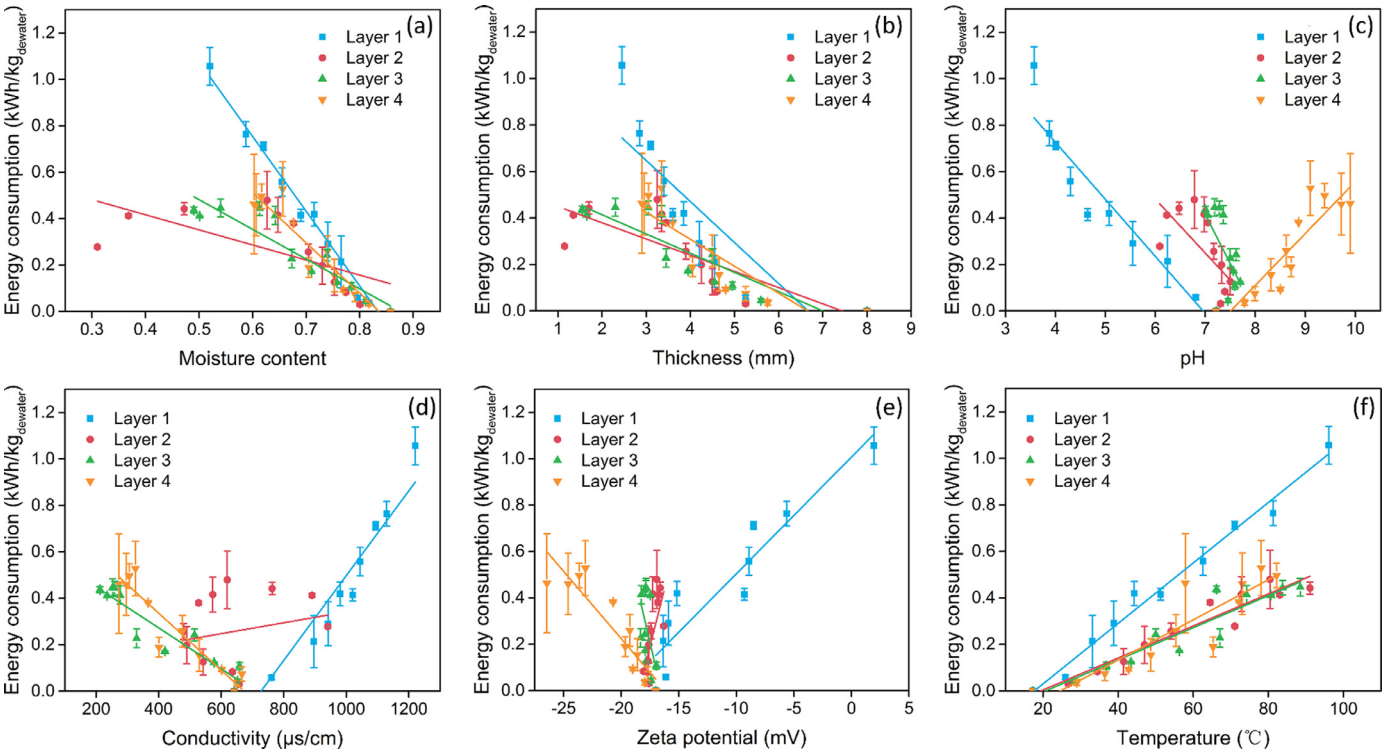

Fig. 5 – Correlations between the energy consumption and sludge characteristics: (a) MC, (b) thickness, (c) pH, (d) conductivity, (e) zeta potential and (f) temperature.

Table 4 – Summary of standardized coefficient (SC) determined by SMLR analysis of ER.

Variable	Layer 1	Layer 2	Layer 3	Layer 4
MC	-	-	0.8001	-
pH	2.6504	0.9982	-	-
Conductivity	-1.6552	-	0.2036	0.9788

Layer 4:

$$R = 3.9519 + \left(6.2431 \times 10^{-7}\right) \times e^{\frac{4569.135}{C}} \quad (16)$$

where MC is the moisture content, H is the thickness, C is the conductivity, and V is the gas volume.

The results of the aforementioned regression equations indicate a variety of significant effects on the ER (layer 1: adj. $R^2 = 0.999$; layer 2: adj. $R^2 = 0.997$; layer 3: adj. $R^2 = 0.998$; layer 4: adj. $R^2 = 0.954$). In addition, the regression equations of SMLR were outlined as follows:

Layer 1:

$$R = 7.4851 + \left(5.7857 \times 10^{-5}\right) \times e^{\frac{46.862}{pH}} - \left(7.8568 \times 10^{10}\right) \times e^{-\frac{26780.761}{C}} \quad (17)$$

Layer 2:

$$R = 4.0591 + \left(2.4106 \times 10^{-12}\right) \times e^{\frac{187.001}{pH}} \quad (18)$$

Layer 3:

$$R = 5.1585 + \left(1.2217 \times 10^{-12}\right) \times e^{\frac{14.869}{MC}} + \left(3.6460 \times 10^{-6}\right) \times e^{\frac{2996.080}{C}} \quad (19)$$

Layer 4:

$$R = 3.9519 + \left(6.2431 \times 10^{-7}\right) \times e^{\frac{4569.135}{C}} \quad (20)$$

where MC is the moisture content and C is the conductivity.

Eq. (17) shows that pH and conductivity can predict the ER in layer 1. However, Table 4 summarized that the standardized coefficient (SC) of pH (SC: 2.6504) was higher than that of conductivity (SC: -1.6552). Thus, pH was the most reliable indicator to predict the ER in layer 1. Eq. (18) shows that pH is the most reliable indicator to predict the ER in layer 2. Meanwhile, Eq. (19) and Table 4 reveal that the MC (SC: 0.8001) was more reliable than conductivity (SC: 0.2036) to predict the ER of layer 3. Finally, Eq. (20) reveals that conductivity is the most reliable indicator to predict the ER in layer 4. These results indicate that the decrease of pH is the main factor affecting the ER of the upper layer (layers 1 and 2), whereas that of the bottom layers were primarily affected by decreasing MC (layer 3) and conductivity (layer 4). As shown in Fig. 2a, the ER of the upper layer was much higher than that of the bottom layer during the later stage of EDW process. Therefore, controlling the pH of the upper layer was the most effective way to decrease the sludge ER.

2.3.2. EC

The regression coefficients of the BEMLR and SMLR analyses for EC (P) are listed in Table 5. The regression equations of the BEMLR are as follows:

Layer 1:

$$P = -0.4019 + 0.0006C + 0.0038V \quad (21)$$

Layer 2:

$$P = -0.4725 + 0.3467MC + 0.0089T \quad (22)$$

Layer 3:

$$P = 0.4285 - 0.6020MC + 0.0041T \quad (23)$$

Layer 4:

$$P = -0.1205 - 0.1389pH - 0.0595\zeta + 0.0066T \quad (24)$$

where MC is the moisture content, C is the conductivity, ζ is the zeta potential, T is the temperature, and V is the gas volume.

The EC regression equations indicate a variety of significant effects on EC (layer 1: adj. $R^2 = 0.990$; layer 2: adj. $R^2 = 0.967$; layer 3: adj. $R^2 = 0.912$; layer 4: adj. $R^2 = 0.955$). In addition, four regression equations of the SMLR were outlined as follows:

Layer 1:

$$P = -0.2296 + 0.0130T \quad (25)$$

Table 5 – Summary of regression coefficients determined BEMLR and SMLR of EC.

Variable	Layer 1			Layer 2			Layer 3			Layer 4		
	BEMLR	SMLR		BEMLR	SMLR		BEMLR	SMLR		BEMLR	SMLR	
	USC	USC	SC	USC	USC	SC	USC	USC	SC	USC	USC	SC
ε	-0.4019	-0.2296	-	-0.4725	-0.4725	-	0.4285	-0.1425	-	-0.1205	0.8258	-
MC	-	-	-	0.3467	0.3467	0.3526	-0.6020	-	-	-	-	-
pH	-	-	-	-	-	-	-	-	-	-0.1389	-	-
Conductivity	0.0006	-	-	-	-	-	-	-	-	-	-0.0012	-0.9503
Zeta potential	-	-	-	-	-	-	-	-	-	-0.0595	-	-
Temperature	-	0.0130	0.9924	0.0089	0.0089	1.2505	0.0041	0.0069	0.9422	0.0066	-	-
Gas volume	0.0038	-	-	-	-	-	-	-	-	-	-	-

USC: unstandardized coefficient; SC: standardized coefficient.

Layer 2:

$$P = -0.4725 + 0.3467MC + 0.0089T \quad (26)$$

Layer 3:

$$P = -0.1425 + 0.0069T \quad (27)$$

Layer 4:

$$P = 0.8258 - 0.0012C \quad (28)$$

where MC is the moisture content, C is the conductivity, and T is the temperature.

Eqs. (25) and (27) reveal that the temperature due to Joule heating was the most reliable indicator for the EC in layers 1 and 3. Meanwhile, Eq. (26) and Table 5 show that temperature (SC: 1.2505) was more reliable than MC (SC: 0.3526) to predict the EC of layer 2. Finally, Eq. (28) reveal that conductivity was the most reliable indicator for the EC in layer 4. Therefore, the temperature of the sludge cake was the most reliable indicator for the EC in layers 1, 2, and 3, whereas that of layer 4 was conductivity.

3. Conclusions

In this study, a sludge cake was divided into four horizontal layers, numbered 1 through 4 from the anode to the cathode. The effects of the sludge characteristics on the ER and EC of each layer during the EDW process were systematically evaluated using correlation and multiple linear regression analyses. Thus, the results provide theoretical guidance for reducing both the ER and EC at the later stage of the EDW process. Notably, the ER and EC were significantly affected by the sludge characteristics. A decreasing pH was the main factor for the increasing ER in layers 1 and 2, while layers 3 and 4 had an increase in ER as a result of the decreasing MC and conductivity, respectively. In addition, the sludge temperature was the most reliable indicator to predict the EC in layers 1, 2, and 3, whereas in layer 4, it was conductivity.

Acknowledgments

This work was supported by the National Natural Science Foundation of China (No. 51608247).

Appendix A. Supplementary data

Supplementary material associated with this article can be found, in the online version, at doi:10.1016/j.jes.2020.09.001.

REFERENCES

Bai, H., Zhu, R., An, H., Zhou, G., Huang, H., Ren, H., Zhang, Y., 2019. Influence of wastewater sludge properties on the performance of electro-osmosis dewatering. Environ. Technol. 40, 2853–2863.

Cai, L., Chen, T., Gao, D., Yu, J., 2016. Bacterial communities and their association with the bio-drying of sewage sludge. Water Res. 90, 44–51.

Citeau, M., Larue, O., Vorobiev, E., 2011. Influence of salt, pH and polyelectrolyte on the pressure electro-dewatering of sewage sludge. Water Res. 45, 2167–2180.

Citeau, M., Larue, O., Vorobiev, E., 2012. Influence of Filter Cell Configuration and Process Parameters on the Electro-Osmotic Dewatering of Sewage Sludge. Sep. Sci. Technol. 47, 11–21.

Citeau, M., Loginov, M., Vorobiev, E., 2016. Improvement of sludge electrodewatering by anode flushing. Dry Technol. 34, 307–317.

Conrardy, J., Vaxelaire, J., Olivier, J., 2016. Electro-dewatering of activated sludge: Electrical resistance analysis. Water Res. 100, 194–200.

Deng, W., Lai, Z., Hu, M., Han, X., Su, Y., 2020. Effects of frequency and duty cycle of pulsating direct current on the electro-dewatering performance of sewage sludge. Chemosphere 243, 125372.

Deng, W., Ma, J., Xiao, J., Wang, L., Su, Y., 2019. Orthogonal experimental study on hydrothermal treatment of municipal sewage sludge for mechanical dewatering followed by thermal drying. J. Clean Prod. 209, 236–249.

Fazeli Sangani, M., Owens, G., Nazari, B., Astaraei, A., Fotovat, A., Emami, H., 2019. Different modelling approaches for predicting titanium dioxide nanoparticles mobility in intact soil media. Sci. Total Environ. 665, 1168–1181.

Guo, X., Qian, X., Wang, Y., Zheng, H., 2018. Magnetic micro-particle conditioning–pressurized vertical electro-osmotic dewatering (MPEOD) of activated sludge: Role and behavior of moisture and organics. J. Environ. Sci. 74, 147–158.

Li, H., Wang, Y., Zheng, H., 2018. Variations of moisture and organics in activated sludge during $Fe^0/S_2O_8^{2-}$ conditioning–horizontal electro-dewatering process. Water Res. 129, 83–93.

Li, Q., Lu, X., Guo, H., Yang, Z., Li, Y., Zhi, S., et al., 2018. Sewage sludge drying method combining pressurized electro-osmotic dewatering with subsequent bio-drying. Bioresource Technol. 263, 94–102.

Lv, H., Liu, D., Zhang, Y., Yuan, D., Wang, F., Yang, J., et al., 2019. Effects of temperature variation on wastewater sludge electro-dewatering. J. Clean Prod. 214, 873–880.

Lv, H., Wang, F., Liu, D., Zhang, Y., Gu, Y., Yuan, D., et al., 2018. Effects of piecewise electric field operation on sludge dewatering: phenomena and mathematical model. Ind. Eng. Chem. Res. 57, 12468–12477.

Lv, H., Xing, S., Liu, D., Wang, F., Zhang, W., Sun, G., et al., 2020. Soluble metal ions migration and distribution in sludge electro-dewatering. Environ. Res. 180, 108862.

Mahmoud, A., Hoadley, A.F.A., Citeau, M., Sorbet, J.M., Olivier, G., Vaxelaire, J., et al., 2018. A comparative study of electro-dewatering process performance for activated and digested wastewater sludge. Water Res. 129, 66–82.

Mahmoud, A., Olivier, J., Vaxelaire, J., Hoadley, A.F.A., 2010. Electrical field: a historical review of its application and contributions in wastewater sludge dewatering. Water Res 44, 2381–2407.

Mahmoud, A., Olivier, J., Vaxelaire, J., Hoadley, A.F.A., 2011. Electro-dewatering of wastewater sludge: influence of the operating conditions and their interactions effects. Water Res. 45, 2795–2810.

Navab-Daneshmand, T., Beton, R., Hill, R.J., Frigon, D., 2015. Impact of joule heating and pH on biosolids electro-dewatering. Environ. Sci. Technol. 49, 5417–5424.

Sha, L., Yu, X., Liu, X., Yan, X., Duan, J., Li, Y., et al., 2019.

Electro-dewatering pretreatment of sludge to improve the bio-drying process. RSC Adv. 9, 27190–27198.
Sha, L., Yu, X., Zhang, Y., Jiang, Q., Liu, X., Wu, Z., et al., 2020. Investigation on the variations of sludge water holding capacity of electro-dewatering process. Environ. Res. 190, 110011.
Sheng, G., Yu, H., Li, X., 2010. Extracellular polymeric substances (EPS) of microbial aggregates in biological wastewater treatment systems: a review. Biotechnol. Adv. 28, 882–894.
Tafti, A.D., Seyyed Mirzaii, S.M., Andalibi, M.R., Vossoughi, M., 2015. Optimized coupling of an intermittent DC electric field with a membrane bioreactor for enhanced effluent quality and hindered membrane fouling. Sep. Purif. Technol. 152, 7–13.
Tang, G.Y., Yang, C., Chai, J.C., Gong, H.Q., 2004. Joule heating effect on electroosmotic flow and mass species transport in a microcapillary. Int. J. Heat. Mass. Tran. 47, 215–227.
Wei, Y., Zhou, X., Zhou, L., Liu, C., Liu, J., 2020. Electro-dewatering of sewage sludge: effect of near-anode sludge modification with different dosages of calcium oxide. Environ. Res. 186, 109487.
Wu, P., Pi, K., Shi, Y., Li, P., Wang, Z., Zhang, H., et al., 2020. Dewaterability and energy consumption model construction by comparison of electro-dewatering for industry sludges and river sediments. Environ. Res. 184, 109335.
Wu, P., Shi, Y., Wang, Z., Xiong, Z., Liu, D., Gerson, A.R., et al., 2019. Effect of electric field strength on electro-dewatering efficiency for river sediments by horizontal electric field. Sci. Total Environ. 647, 1333–1343.
Yang, Z., Lu, X., Zhang, S., Zhang, K., Zhi, S., Guo, H., et al., 2018. Pressurized electro-dewatering of activated sludge: analysis of electrode configurations (anode). Waste Manage 81, 157–167.
Yeung, A.T., Hsu, C., Menon, R.M., 1997. Physicochemical soil-contaminant interactions during electrokinetic extraction. J. Hazard. Mater. 55, 221–237.
Yu, W., Yang, J., Wu, X., Gu, Y., Xiao, J., Yu, J., et al., 2017. Study on dewaterability limit and energy consumption in sewage sludge electro-dewatering by in-situ linear sweep voltammetry analysis. Chem. Eng. J. 317, 980–987.
Zhang, S., Yang, Z., Lv, X., Zhi, S., Wang, Y., Li, Q., et al., 2017. Novel electro-dewatering system for activated sludge biosolids in bench-scale, pilot-scale and industrial-scale applications. Chem. Eng. Res. Des. 121, 44–56.
Zheng, X., Jiang, Z., Ying, Z., Song, J., Chen, W., Wang, B., 2020. Role of feedstock properties and hydrothermal carbonization conditions on fuel properties of sewage sludge-derived hydrochar using multiple linear regression technique. Fuel 271, 117609.